Assessment of impact of Hysteresis phenomenon on Magnitude-Frequency Analysis for Godavari River basin, India

Shobhit Maheshwari (2017cez0003@iitrpr.ac.in) and Sagar R. Chavan (sagar@iitrpr.ac.in)
Department of Civil Engineering, Indian Institute of Technology, Ropar 140001, India

AGU FALL MEETING
Online Everywhere | 1–17 December 2020

INTRODUCTION

- Magnitude-Frequency Analysis (MFA) provides a mathematical framework to determine "effective discharge" (i.e. discharge responsible for transportation of majority of sediments from a basin over a long period of time) by maximizing transport effectiveness function (TE).
- TE of a given discharge is the product of frequency of discharge and corresponding sediment load.
- The discharge was assumed to follow lognormal distribution and rating curves (between discharge and sediment load) developed for total, rise and fall (to check hysteresis), monsoon, monsoon rise and fall and individual months.
- MFA based effective discharges calculated at 16 Gauges in Godavari River basin, India and these estimates can find use in the effective planning and functioning of dams/reservoirs.

STUDY AREA

- Godavari River is India's second longest river whose basin spreads over Indian states of Maharashtra, Andhra Pradesh, Chhattisgarh and Odisha.
- It has a total catchment area of 312,812 km2 and covers for nearly 9.5% of the total geographical area of India.
- The total length of the river from its origin to outfall into the Bay of Bengal is 1,465 km.

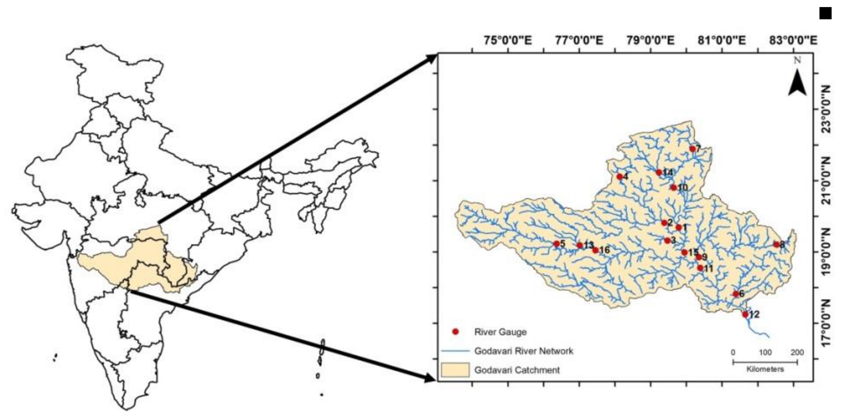

- Figure 1: Locations of the 16 Gauges of Godavari River basin, India considered in this study (numbers correspond to IDs of the Stream Gauges).

ID #	River Gauge	Elevation (m)	Area (km^2)	Length of record (days)	Mean Discharge (m^3/sec)
1	'Ashti'	141.4	49056.3	10957	682.28
2	'Bamni'	158	45256.5	13149	368.83
3	'Bhatpalli'	156	3129.1	5113	29.61
4	'Bishnur'	286	4880.6	4384	15.80
5	'Dhalegaon'	398	29763.9	4748	87.67
6	'Konta'	45	19703.5	11688	472.50
7	'Kumhari'	289	7401.9	2922	90.20
8	'Nowrangpur'	560	2976	10227	89.99
9	'Pathagudem'	104	37522.6	12418	739.56
10	'Pauni'	218.5	33695.1	8036	396.76
11	'Perur'	79	261513.1	14611	2183.51
12	'Polavaram'	26	300046.7	14245	2600.32
13	'Purna'	358	14963.2	4018	47.56
14	'Satrapur'	263.3	10962.7	5478	67.45
15	'Tekra'	95.1	104670.7	11322	1182.19
16	'Yelli'	352	52458.1	2192	191.38

- Table 1: River basin characteristics.

METHODOLOGY

- The sediment load carried through a stream network can be affected by the variability in stream flow occurring during different months or seasons (i.e. time scales) and consequent hysteresis phenomenon.
- Prediction of sediment load can be improved by constructing separate rating curves for various time scales.

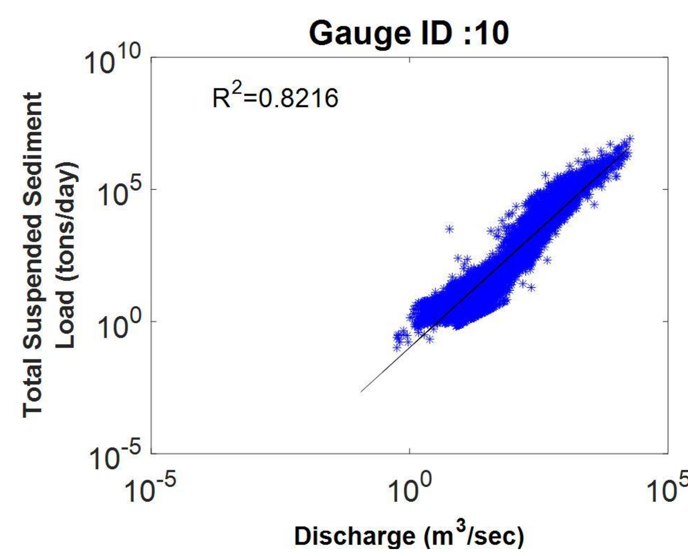

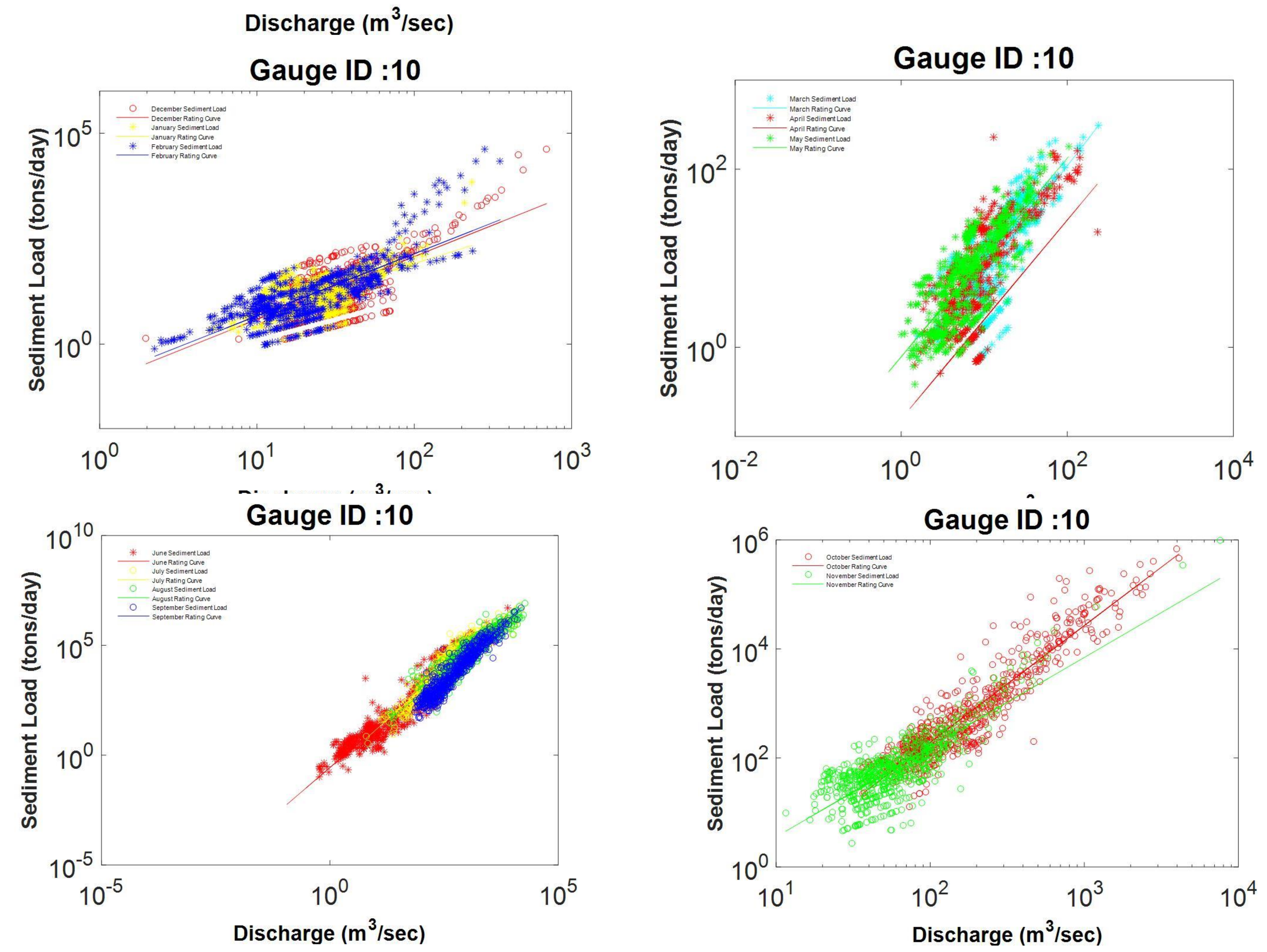

- Figure 2: Log-Log plots of power-law relationship between total suspended sediment load and discharge observed for Gauge ID: 10 (for brevity, single gauge is shown in figure).
- Figure 3: Log-Log plots of power-law relationship between individual month suspended sediment load and discharge observed for Gauge ID: 10 (Shown by grouping months according to seasons).

- Daily discharge was assumed to follow log normal distribution.
- TE function was developed for total, both stages (rise and fall), monsoon season, monsoon with stages and twelve months data.
- Effective discharges were calculated for these eighteen cases at 16 Gauges.

$$f(q_t) = \frac{1}{q_t \beta_t \sqrt{2\pi}} e^{-(\ln q_t - \alpha_t)^2 / 2\beta_t^2}$$

$$S_t = a_t (q_t)^{b_t}$$

$$\mathrm{TE} = \frac{a_t (q_t)^{b_t}}{q_t \beta_t \sqrt{2\pi}} e^{-(\ln q_t - \alpha_t)^2 / 2\beta_t^2}$$

$$Q_e^t = \exp((b_t - 1)\beta_t^2 + \alpha_t)$$

RESULTS

- In case of total suspended sediment data, clockwise hysteresis was observed in 13 Gauges whereas in rest 3 Gauges (4, 6 and 9), no effect was found.
- For monsoon data, clockwise hysteresis was observed in 12 Gauges whereas in remaining 4 Gauges (1, 14, 15 and 16), no effect was found.

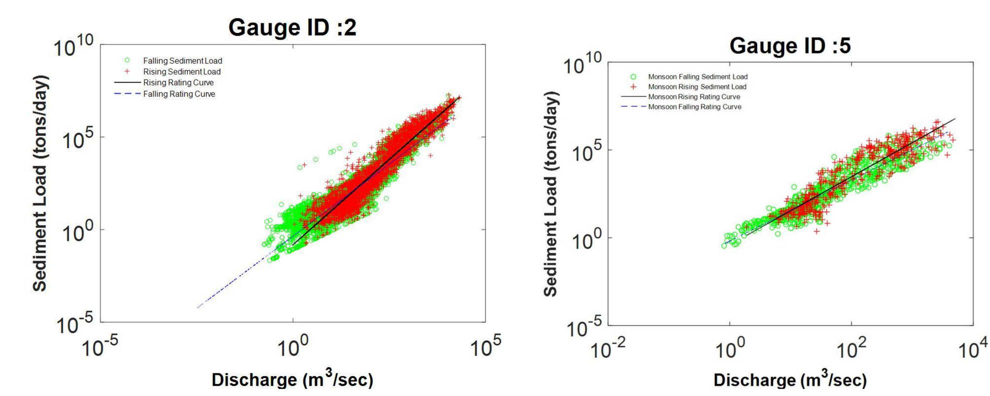

- Effect of hysteresis by dividing the data into two stages: rising and falling.

ID #	Q_e^{Total} (m^3/s)	Q_e^{Rise} (m^3/s)	Q_e^{Fall} (m^3/s)	Q_e^{Mon} (m^3/s)	$Q_e^{Mon-Rise}$ (m^3/s)	$Q_e^{Mon-Fall}$ (m^3/s)
1	1370.09	3905.13	695.51	3364.51	4251.85	2620.12
2	863.99	3546.56	353.77	2849.86	4586.64	1740.98
3	19.36	94.02	10.84	64.70	111.04	39.62
4	28.15	43.64	17.34	24.20	50.64	14.75
5	438.82	458.93	225.75	904.15	1903.65	426.01
6	736.78	802.97	687.03	1231.47	1515.20	1027.80
7	186.01	471.21	79.70	333.75	641.16	191.73
8	217.85	335.45	141.98	303.78	390.62	233.34
9	2834.54	6019.67	1668.83	2530.54	3418.05	2018.86
10	1231.33	5124.42	532.66	2341.20	3057.84	1667.91
11	7969.56	17738.53	4881.64	12246.12	15872.71	9817.79
12	6840.52	8693.38	5791.67	12290.47	15673.37	10025.31
13	38.30	161.55	18.41	244.57	611.99	97.16
14	52.90	238.33	28.47	279.89	476.12	177.46
15	5732.02	18466.27	2759.71	7372.57	9542.85	5620.59
16	344.59	694.16	221.89	1629.72	2766.64	957.51

- Table 2: Estimates of effective discharges for total, staging, monsoon and monsoon staging data.

ID #	Q_e^{Jan} (m^3/s)	Q_e^{Feb} (m^3/s)	Q_e^{Mar} (m^3/s)	Q_e^{Apr} (m^3/s)	Q_e^{May} (m^3/s)	Q_e^{Jun} (m^3/s)	Q_e^{Jul} (m^3/s)	Q_e^{Aug} (m^3/s)	Q_e^{Sep} (m^3/s)	Q_e^{Oct} (m^3/s)	Q_e^{Nov} (m^3/s)	Q_e^{Dec} (m^3/s)
1	38.52	30.85	22.04	10.19	8.32	174.32	2804.42	3999.49	2906.25	868.20	143.15	43.20
2	27.13	24.09	12.12	5.00	4.16	2846.44	2312.81	3844.14	2424.91	521.14	55.31	32.40
3	4.75	4.57	4.59	3.28	3.03	15.52	39.80	111.32	70.20	25.43	8.63	4.64
4	0.38	0.26	0.06	0.05	309.69	51.94	25.74	41.94	23.96	14.63	4.36	0.53
5	15.50	17.77	11.84	3.50	5.39	6276.85	463.84	1166.76	1189.37	304.34	34.35	20.72
6	184.63	174.59	165.31	156.36	148.64	351.26	909.94	1702.65	1143.47	608.06	308.48	218.18
7	22.93	16.56	3.90	2.34	0.71	28.42	263.55	420.11	319.12	27.19	22.59	50.56
8	48.14	25.04	34.34	36.06	55.99	87.52	258.35	368.40	276.49	98.34	42.92	44.42
9	46.32	21.17	10.00	7.69	10.07	1538.31	1600.05	3866.24	2312.07	740.83	176.99	66.37
10	25.64	29.17	13.55	8.05	5.68	698.92	1878.77	2617.16	1947.61	461.81	80.40	37.42
11	173.60	142.61	98.60	58.07	50.41	1271.10	8843.58	13016.33	11282.50	4207.54	829.98	324.29
12	395.50	336.26	289.11	238.21	223.22	1221.11	8898.50	14724.39	11397.04	4921.32	1061.83	502.32
13	6.47	6.84	4.18	3.54	3.49	52.58	159.95	238.04	356.69	57.52	12.84	7.79
14	8.11	6.32	4.86	3.05	2.97	25.47	264.23	304.77	272.73	61.90	16.71	9.04
15	74.59	71.02	37.29	18.10	12.14	913.66	6422.97	8004.28	6138.86	1814.08	303.39	116.30
16	29.92	31.01	24.30	12.12	14.93	199.64	457.14	2392.87	3061.61	597.24	57.26	58.49

- Table 3: Estimates of effective discharges for individual month data.

DISCUSSION

- Most of the stream gauges depict clockwise hysteresis in case of total as well as monsoon suspended sediment data.
- None of the Gauge shows anti-clockwise hysteresis in both set of data.
- Prediction of sediment load can be improved by fitting separate power law for different sets of data (months, seasons and stages).
- Effective discharge estimates were found to be higher in case of rising data sets (for total and monsoon).
- Impact of change in flood event due to monsoon or rainy season is clearly visible in the estimates of effective discharge for individual months.

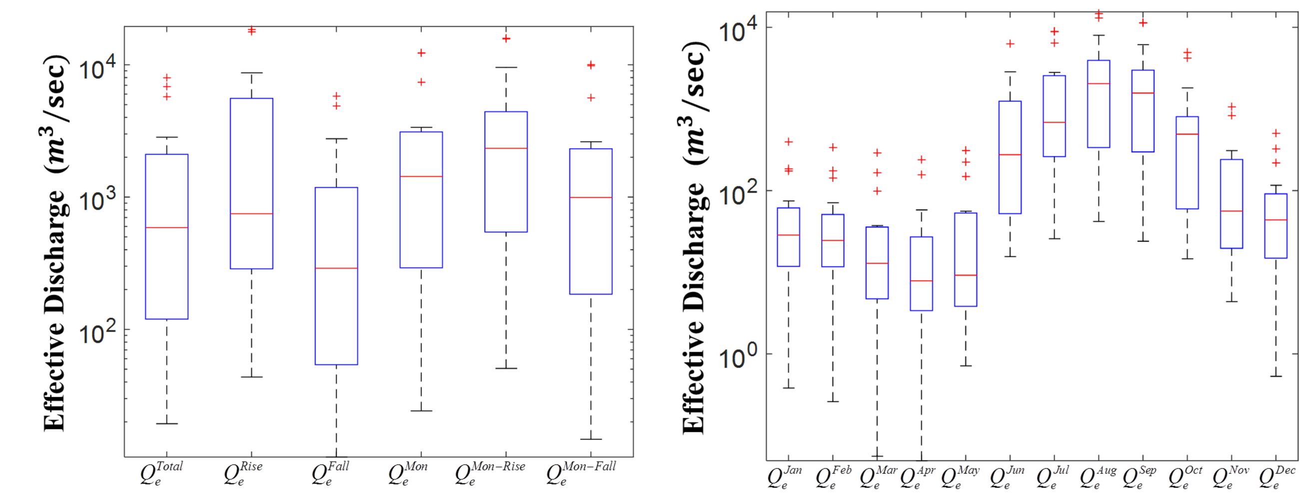

- Box plots showing variation in the estimates of effective discharge for different sets of data ,

CONCLUSIONS

- Estimates of effective discharge for different stages can be helpful to understand the impact of hysteresis which ultimately related to geomorphology of the catchment.
- Effective discharge is directly related to the exponent of power-law relationship and standard deviation of log transformed discharge data.
- Variation of these two factors over different months (due to change in flood and landscape) leads to the varied estimates of effective discharge estimates over individual months.
- Further, it was inferred that power law relationship between discharge and sediment load can be improved by dividing the data for different months, seasons and stages.
- The results of this study can find use in the effective planning and functioning of dams/reservoirs.

REFERENCES

- Basso, S., Frascati, A., Marani, M., Schirmer, M., Botter, G., 2015. Climatic and landscape controls on effective discharge 8441–8447. https://doi.org/10.1002/2015GL066014.
- Goodwin, P., 2004. Analytical Solutions for Estimating Effective Discharge. J. Hydraul. Eng. 130, 729–738. https://doi.org/10.1061/(asce)0733-9429(2004)130:8(729).
- Maheshwari, S., Chavan, S.R., 2019. Magnitude–frequency analysis to assess effective discharge at daily and monthly timescales in South Indian River basins. ISH J. Hydraul. Eng. 00, 1–10. https://doi.org/10.1080/09715010.2019.1603088.
- Nash, D.B., 1994. Effective sediment-transporting discharge from magnitude-frequency analysis, J. Geol., 102(1), 79–95, doi:10.1086/629649.
- Syvitski, J.P., Morehead, M.D., Bahr, D.B., Mulder, T., 2000. Estimating fluvial sediment transport : The rating parameters parameters (a and b) are defined by a power law relating discharge values of a river mathematical concentration is inversely proportional to the long-term. Water Resour. 36, 2747–2760. https://doi.org/10.1039/C7RE00129K.
- Vogel, R.M., Stedinger, J.R., Hooper, R.P., 2003. Discharge indices for water quality loads. Water Resour. Res. 39, 1–9. https://doi.org/10.1029/2002WR001872.
- Wolman, M.G., Miller, J.P., 1960. Magnitude and frequency of forces in geomorphic processes, J. Geol., 68(1), 54–74, doi:10.1086/626637.